IEEE Access
Multidisciplinary | Rapid Review | Open Access Journal

Received March 11, 2018, accepted April 12, 2018, date of publication April 20, 2018, date of current version May 24, 2018.

Digital Object Identifier 10.1109/ACCESS.2018.2828126

Sub-Graph Based Joint Sparse Graph for Sparse Code Multiple Access Systems

KE LAI[1], LEI WEN[1,2], JING LEI[1], PEI XIAO[2], (Senior Member, IEEE), AMINE MAAREF[3], (Senior Member, IEEE), AND MUHAMMAD ALI IMRAN[4], (Senior Member, IEEE)

[1]Department of Communication Engineering, College of Electronic Science, National University of Defence Technology, Changsha 410073, China
[2]Institute for Communication Systems, Home of the 5G Innovation Centre, University of Surrey, Guildford GU2 7XH, U.K.
[3]Huawei Technologies, Ottawa, ON K2K3J1, Canada
[4]School of Engineering, University of Glasgow, Glasgow G12 8QQ, U.K.

Corresponding author: Lei Wen (newton1108@126.com)

This work was supported in part by Huawei Technologies Company Ltd., Ottawa, Canada, in part by the National Natural Science Foundation of China under Grant 61502518, Grant 61702536, and Grant 61372098, in part by the National Defense Technology Foundation under Grant 3101168, in part by the Hunan Natural Science Foundation under Grant 2017JJ2303, and in part by the Natural Science Research Project of the National University of Defense Technology Research of new multiple access techniques based on joint sparse graph.

ABSTRACT Sparse code multiple access (SCMA) is a promising air interface candidate technique for next-generation mobile networks, especially for massive machine-type communications. In this paper, we design a low-density parity-check (LDPC) coded SCMA detector by combining the sparse graphs of LDPC and SCMA into one joint sparse graph (JSG). In our proposed scheme, the SCMA sparse graph defined by small size indicator matrix is utilized to construct the JSG, which is termed as sub-graph-based JSG of SCMA (SG-JSG-SCMA). In this paper, we first study the binary-LDPC coded SG-JSG-SCMA system. To combine the SCMA variable node and LDPC variable node into one joint variable node, a non-binary LDPC (NB-LDPC) coded SG-JSG-SCMA is also proposed. Furthermore, to reduce the complexity of NB-LDPC coded SG-JSG-SCMA, a joint trellis representation (JTR) is introduced to represent the search space of NB-LDPC coded SG-JSG-SCMA. Based on JTR, a low complexity joint trellis-based detection and decoding algorithm is proposed to reduce the computational complexity of the NB-LDPC coded SG-JSG-SCMA system. According to the simulation results, SG-JSG-SCMA brings significant performance improvement compare with the conventional receiver using the disjoint approach, and it can also outperform a turbo-structured receiver with comparable complexity. Moreover, the joint approach also has advantages in terms of processing latency compare with the turbo approaches.

INDEX TERMS 5G, SCMA, LDPC, joint trellis representation, joint receiver, multiuser channels.

I. INTRODUCTION

Since the commercialization of 4th generation (4G) mobile networks, researchers have focused on the new air-interface technology, which is more efficient and reliable, to meet the demands of the 5th generation (5G) mobile networks [1]. To further increase the spectral efficiency, non-orthogonal multiple access (NOMA) is proposed as an alternative to conventional orthogonal multiple access (OMA). The first scheme of NOMA is referred as power domain NOMA [2], and its application in LTE as well as 5G systems is studied in [3]. SCMA [4] is a code domain NOMA that is considered to be a promising 5G candidate due to its excellent ability to support massive quantities of users under heavily overloading conditions.

The first scheme of code domain NOMA was referred as low density signature (LDS) [5]. Motivated by multi-carrier CDMA (MC-CDMA), sparsity is introduced to the spreading matrix in LDS, and it performs well under overloading conditions. Later, Beek and Popovic [6], proposed to design the spreading matrices through rotation to further improve the performance of LDS. Hoshyar *et al.* [7] combined LDS with orthogonal frequency division multiplexing (LDS-OFDM), which can achieve a superior performance to orthogonal frequency division multiple access (OFDMA) [7]. In fact,

SCMA, which is characterized by codebook design and different constellation mapping, is an extension of LDS [4]. Compared with LDS, SCMA directly maps code bits to a complex symbol. In order to obtain a better performance, Taherzadeh *et al.* [8] proposed to obtain shaping gain through rotating constellation in codebook design. Similar to LDS, message passing algorithm (MPA) can be used in a SCMA detector as well.

Since the LDS and SCMA were proposed, their simplified detection algorithms have attracted much attention [9]–[14]. However, to reduce receiver processing latency without performance loss and further improve the error rate performance, novel receiver structure should be also taken into consideration. In [15], an iterative Turbo structured receiver for a Turbo coded LDS system is proposed, which can achieve superior performance compare with conventional individual receiver. In [16]–[19], we designed a joint sparse graph for a low-density parity-check (LDPC) coded LDS-OFDM system and CDMA system, which is termed as JSG-LDS and JSG-CDMA, respectively. The proposed scheme brings about 1.5-1.8dB performance improvement at bit error rate (BER) of 10^{-5} compared with a Turbo-style iterative receiver. In [20], an iterative Turbo-style SCMA receiver was proposed, which can achieve a better performance than a separate one with comparable computational complexity. A joint detection algorithm for SCMA system is proposed in [21]. In [22], a joint receiver that combines SCMA and downlink MIMO system is presented.

Inspired by the message exchange strategy in a LDPC coded large MIMO system which is proposed in [23], a sub-graph based joint sparse graph (SG-JSG) is proposed to perform joint detection and decoding for a LDPC[1] coded SCMA system. The SG-JSG is constituted by SCMA Tanner graphs [25] with 4 function nodes (FNs) and 6 SVNs, which is called 4-6 SCMA or 4-6 SSG for brevity in this paper. After linking the B-LDPC sparse graphs (B-LSGs) and SSGs into a SG-JSG, the message passing algorithm (MPA) will operate on the SG-JSG with only outer iterations. However, as the MPA performs on the B-LSG at the bit-level, while the MPA performs on the SSG at the symbol-level, the LVNs and SVNs are separated on the SG-JSG. To combine the LVNs and SVNs into a JVN, NB-LDPC code is introduced to SG-JSG-SCMA system; hence, the NB-LDPC sparse graph (NB-LSGs) and SSGs can be directly linked through JVNs. However, it is computationally expensive when applying NB-LDPC codes to the SG-JSG-SCMA system. Therefore, a simplified algorithm based on JTR that only uses partial messages is proposed, i.e., the JTDD algorithm. The search space of JTDD can be significantly reduced with a few extra calculations.

The main novelties and contributions of this paper are listed as follows:

1) We combine two kinds of bipartite graph, including SCMA and LDPC bipartite graph, into one graph model, which is referred as SG-JSG-SCMA. Such a receiver that can perform detection and decoding simultaneously has never been proposed for SCMA. Additionally, to the best of our knowledge, a JSG that consists of sub-graphs of multiple access system and channel decoder is also a novel graph model in the design of channel coded detector.

2) MPA over SG-JSG are modified to adopt to B-LDPC and NB-LDPC coded SG-JSG-SCMA system. Typically, a separate receiver performs MPA and BP independently for SCMA detector and LDPC decoder, respectively [26]. As for Turbo-style receiver, the messages pass through Turbo structure [26]. However, SG-JSG-SCMA is a novel receiver structure based on SG-JSG, where detection and decoding are performed jointly on the entire graph; hence, the MPA should be modified so that the information of each user can be detected.

3) A trellis representation is introduced to the update of FNs in SCMA. Furthermore, we extend it to a JTR which can link SCMA trellis and NB-LDPC trellis together. Based on JTR, a simplified algorithm that only uses partial messages are proposed to reduce the complexity of a NB-LDPC coded SG-JSG-SCMA system. To compensate the performance loss, the information feedback strategy with Gaussian forcing and some compensation methods are introduced. Such a simplified detection and decoding algorithm based on MPA and SG-JSG has never been reported.

4) To further illustrate the validity and advantages of our proposed scheme, we analyze the SG-JSG-SCMA system from several perspectives. The results show that the SG-JSG-SCMA is a well-performed receiver compare to the existing ones.

The rest of this paper is structured as follows. In Sec. 2, we introduce the system model of uplink SCMA and the graph model of SG-JSG-SCMA, respectively. Sec. 3 presents the modified MPA in the SG-JSG-SCMA system. JTR and JTDD for the NB-LDPC coded SG-JSG-SCMA are introduced in Sec. 4. The simulation results and discussions are presented in Sec. 5. Sec. 6 concludes this paper. A summary of abbreviations used in this paper is presented in Table 1.

II. SYSTEM MODEL

A brief introduction of uplink SCMA and the graph model of SG-JSG-SCMA are presented in this section.

A. SPARSE CODE MULTIPLE ACCESS

We consider the uplink transmissions where J single-antenna users transmit to the same base station (BS).

At the transmitter in Fig. 1, the functional blocks are similar to that of LDS-OFDM. However, the information bits of each user are directly mapped to complex signals through certain codebooks in the SCMA encoder, then the signals superpose at the transmitter and transmitting with OFDMA sub-carriers. Upon receiving the superimposed signals at the

[1] It is worth mentioning that LDPC codes have been adopted in the 5G new radio standards for data channels. A comprehensive and detailed review of its graph model and design rule is reported in [24].

TABLE 1. Summary of main abbreviations and key notations.

4-6 SCMA	SCMA system with 4 function nodes and 6 variable nodes	B-LDPC	Binary LDPC codes
NB-LDPC	Non-binary LDPC codes	JSG	Joint sparse graph
LSG	LDPC sub-graph	B-LSG	Binary LSG
NB-LSG	Non-binary LSG	SSG	SCMA sub-graph
SG-JSG	Sub-graph based joint sparse graph	SG-JSG-SCMA	Sub-graph based joint sparse graph for SCMA
CN	Parity-check nodes	FN	Function nodes
LVN	LDPC variable nodes	SVN	SCMA variable nodes
JVN	Joint variable nodes	JTR	Joint trellis representation
JTDD	Joint trellis detection and decoding	FFT-BP	Fast Fourier transformation based belief propagation
N	Number of SSGs in SG-JSG	M	Code length of LDPC codes
J	Number of users	K	Number of transmitted OFDMA subcarriers
L	Number of CNs in LSGs	$\boldsymbol{F_{K\times J}}$	Indicator matrix of low density signature
$v_{n,j}$	jth SVN at nth SSG	$Lv_{k,m}$	mth LVN at kth LSG
$f_{n,k}$	kth FN at nth SSG	$p_{k,l}$	lth CN at kth LSG
d_p	Degree of CN in a LSG	d_f	Degree of FN in a SSG
ξ_k^n	Set of SVNs that kth FN connects to in nth SSG	ϕ_l^j	Set of LVNs that lth CN connects to in jth LSG
$\xi_k^n \backslash j$	Set of SVNs that connects to kth FN in nth SSG (excluding $v_{n,j}$)	$d_{n,k}(\boldsymbol{x})$	Euclidean distance between kth received signals in nth SSG and SCMA codewords
$I_{f_{n,j}\to v_{n,k}}$	Messages that deliver from $f_{n,j}$ to $v_{n,k}$	$I_{Jv_{j,m}\to p_{k,l}}$	Messages that deliver from $Jv_{j,m}$ to $p_{k,l}$
$I_{p_{k,l}\to Lv_{j,m}}$	Messages that deliver from $p_{k,l}$ to $Lv_{j,m}$	$I_{Jv_{j,m}\to f_{n,j}}$	Messages that deliver from $Jv_{j,m}$ to $f_{n,j}$

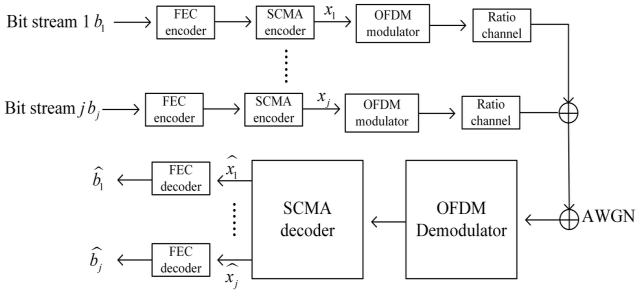

FIGURE 1. Block diagram for SG-JSG-SCMA transmitter.

receiver, the MPA is applied to detect the information transmitted by each user.

Similar to LDS, SCMA can be defined by an sparse indicator matrix $\boldsymbol{F}_{K\times J}$ that has d_f non-zero elements in each row and d_u non-zero elements in each column. $\boldsymbol{F}_{K\times J} = (\boldsymbol{f_1}, \boldsymbol{f_2}, \ldots, \boldsymbol{f_J})$, where $\boldsymbol{f_j} = (f_{j,1}, f_{j,2}, \cdots, f_{j,k})^T$. Due to the sparsity of $\boldsymbol{F}_{K\times J}$, SCMA can be represented by a Tanner graph [25].

For a conventional 4-6 SCMA system, the indicator matrix can be represented as:

$$\boldsymbol{F}_{4\times 6} = \begin{bmatrix} 0 & 1 & 1 & 0 & 1 & 0 \\ 1 & 0 & 1 & 0 & 0 & 1 \\ 0 & 1 & 0 & 1 & 0 & 1 \\ 1 & 0 & 0 & 1 & 1 & 0 \end{bmatrix}. \tag{1}$$

The non-zero elements in $\boldsymbol{F}_{4\times 6}$ represent the connection between SVNs and FNs, which indicates that the jth user is spread by the kth chip. We assume that the numbers of non-zeros in each column and each row are the same. Therefore, the received signal at BS can be written as:

$$\boldsymbol{y}^j = \sum_{j=1}^{J} diag(\boldsymbol{h}^j)\boldsymbol{x}_j + \boldsymbol{z}, \tag{2}$$

where $diag(\boldsymbol{h}^j)$ is a diagonal matrix, vector $\boldsymbol{x}_j$ is the SCMA codeword of the jth user, $\boldsymbol{y^j} = [y_1^j, y_2^j, \cdots, y_K^j]^T$ is the signal vector received by jth users, $\boldsymbol{h}^j = [h_1^j, h_2^j, \cdots, h_K^j]^T$ is the channel gain between user j and the BS, and $\boldsymbol{z}$ is Gaussian noise with variance δ^2.

B. GRAPH MODEL OF B-LDPC CODED SG-JSG-SCMA

As discussed above, SCMA detector and LDPC decoder can be both represented by sparse graphs. Moreover, in the Turbo-style receiver, the output of channel decoder is utilized as *a priori* information of SCMA detector in the next iterations. If the extrinsic information is exchanged between SCMA detector and the LDPC decoder, the error rate performance can be improved.

As shown in Fig. 2, a SG-JSG-SCMA receiver for a B-LDPC coded 4-6 SCMA is depicted. In contrast to JSG-LDS, the SG-JSG-SCMA consists of four types of nodes: FNs, SVNs, LVNs and parity check nodes (CNs). In this paper, N and M denotes the number of data symbols and code length, respectively. Note that N is also the number of SSGs in SG-JSG-SCMA. L represents the number of CN. Let $v_{n,j}$ ($n \in [1, N], j \in [1, J]$) be the $v_{n,j}$th SVN in nth SSG corresponding to the data of jth user; $Lv_{k,m}$ ($k \in [1, K], m \in [1, M]$) is the mth LVN of kth user. It should be noted that the symbol-level MPA is used to detect SCMA symbols; whereas belief propagation (BP), which is a bit-level MPA, is used to decode B-LDPC. Therefore, a mapping between the messages of SVN and LVN is necessary. In 4-point (16-point) SG-JSG-SCMA, each SVN connects to two

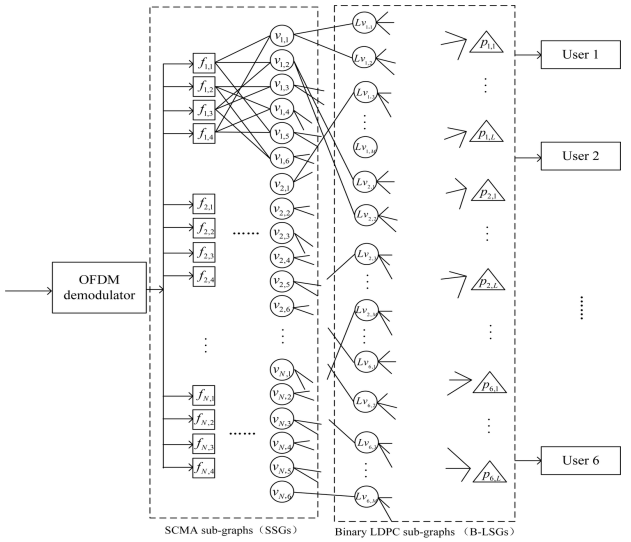

FIGURE 2. Block diagram for SG-JSG-SCMA receiver.

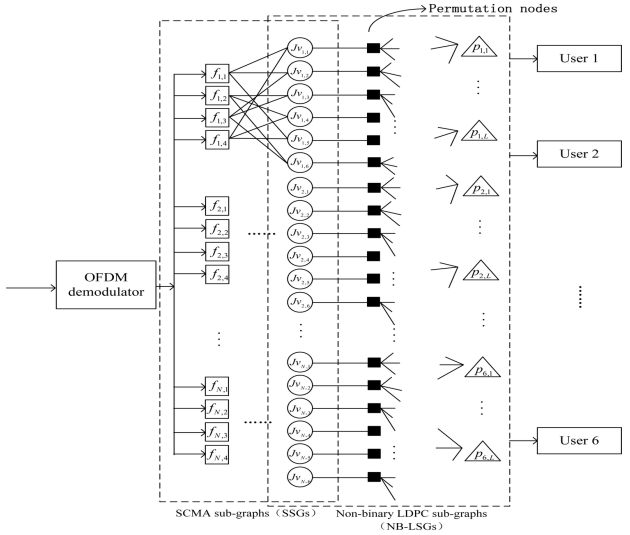

FIGURE 3. Block diagram of NB-LDPC coded SG-JSG-SCMA.

(resp. four) LVNs. For example, the nodes $v_{n,1}$ ($n \in [1, N]$) connect to the nodes $Lv_{1,2m-1}$ and $Lv_{1,2m}$ ($m \in [1, \lceil \frac{M}{2} \rceil]$); hence, the first user's data is decoded in the 1st B-LSG. As such, the SSGs and B-LSGs are linked together.

Each SSG corresponds to four OFDMA sub-carriers, therefore, the number of SSGs depends on the length of transmitted data and number of sub-carriers. As for LSG, the number of LSG totally depends on J, which is the number of users. By combining SSG and LSG into one JSG, the SG-JSG-SCMA integrates the inner iterations of both the SCMA detector and B-LDPC decoder. Therefore, only the outer iterations are necessary for the proposed joint detector and decoder.

With the joint detection and decoding, the FNs in SSGs and CNs in LSGs update simultaneously at first. Then, the SSGs and B-LSGs update their variable nodes separately. The messages are subsequently exchanged between LVNs and SVNs. Iterations go on until the decoded codewords satisfy the parity-check equations in each LSG.

C. GRAPH MODEL OF NB-LDPC CODED SG-JSG-SCMA

As shown in Fig. 2, the LVNs and SVNs are independent; hence, a connected model which includes mapping and de-mapping for the information between LVNs and SVNs is necessary in a B-LDPC coded SG-JSG-SCMA. To combine the SVN and LVN to a JVN without connected model, NB-LDPC code is introduced to construct the SG-JSG-SCMA. Note that NB-LDPC codes that define over $GF(4)$ and $GF(16)$ are utilized on 4-point SCMA and 16-point SCMA, respectively. As such, the dimension of SCMA messages and NB-LDPC code messages are matched. Therefore, the LVNs and SVNs are merged into JVN without extra connected model and calculations.

The graph model of NB-LDPC coded SG-JSG-SCMA is illustrated in Fig. 3. Since the detection of SCMA and the decoding of NB-LDPC are both symbol-level MPA, only JVNs are presented in the graph model of NB-LDPC coded SG-JSG-SCMA. Additionally, as the transformation of symbols is necessary in the decoding of NB-LDPC codes to satisfy the parity-check equations, permutation nodes (PNs) should be added to the SG-JSG.

The process of the messages update in a NB-LDPC coded SG-JSG-SCMA is the same as B-LDPC coded SG-JSG-SCMA. However, as mentioned earlier, messages exchanging between SVN and LVN is unnecessary in the NB-LDPC coded SG-JSG-SCMA as a symbol-level decoder is implemented. In fact, there is another method to combine LVNs and SVNs, i.e., to transform symbol-level SCMA detector into a bit-level SCMA detector. Nonetheless, such a bit-level SCMA detector is related to multi-layer Tanner graph [27], which is complexity expensive for practical implementations.

III. SG-JSG-SCMA BASED MESSAGE PASSING ALGORITHM

In this section, the modified version of B-LDPC and NB-LDPC coded SG-JSG-SCMA based joint detection and decoding algorithm are presented, respectively.

A. MODIFIED MPA IN B-LDPC CODED SG-JSG-SCMA

1) FUNCTION NODES UPDATE

In probability domain, the message sent from FN $f_{n,k}$ to SVN $v_{n,j}$ can be written as:

$$I_{f_{n,j}\to v_{n,k}}(\boldsymbol{x}_k) = \frac{1}{2\pi N_0} \cdot \exp\left(\frac{1}{2N_0 d_{n,k}(\boldsymbol{x})}\right) \cdot \prod_{u\in\xi_k^n\backslash j} I_{v_{n,u}\to f_{n,j}}(\boldsymbol{x}_k), \quad (3)$$

where N_0 is the variance of noise, and $d_{n,k}(\boldsymbol{x})$ is an Euclidean distance related value which is given by:

$$d_{n,k}(\boldsymbol{x}) = \frac{1}{\sigma^2}\|y_{n,k} - \sum_{k\in\xi_k^n} h_{j,k}x_{j,k}\|, \tag{4}$$

and $y_{n,k}$ is the received signal in nth SSG sub-carrier k; $x_{j,k}$ is the kth component of SCMA codeword $\boldsymbol{x}_j$. $\xi_k^n = \{j|f_{j,k} \neq 0\}$ for $n = 1, \cdots, N$, $f_{j,k}$ denotes the non-zero elements in the indicator matrix; hence, ξ_k^n is a node set whose elements connect to kth FN in nth SSGs. It should be noted that (3) is a general version of FN update, which is satisfied for any given low density spreading matrix in SCMA.

2) PARITY-CHECK NODES UPDATE

The CN update in SG-JSG is the same as the LDPC decoding. Similarly, we define a node set ϕ_l^j whose elements are the nodes that connect with lth CN in jth B-LSG. Note that the update of CN is independent of each B-LSG which is similar to the FN update in SSG. Therefore, the update of CNs can be written as:

$$I_{p_{k,l}\to Lv_{k,i}} = 2\times T^{-1}\left(\prod_{\forall m\neq i: Lv_m\in\phi_l^j} T(I_{Lv_{k,m}\to p_{k,l}})\right), \tag{5}$$

where

$$T(x) = \tanh(x) = \frac{e^x - e^{-x}}{e^x + e^{-x}}, \tag{6}$$

and

$$T^{-1}(x) = \tanh^{-1}(x) = \frac{1}{2}\cdot\log\left(\frac{1+x}{1-x}\right). \tag{7}$$

It should be noted that the messages are defined over the logarithm domain, which can be also denoted as log-likelihood ratio (LLR).

3) VARIABLE NODES UPDATE

Unlike JSG-LDS, the update of variable nodes in SG-JSG is more complicated since there are two kinds of variable nodes in JSG-SCMA. Therefore, the process of variable node update can be split into two parts:

a) SCMA VARIABLE NODES UPDATE

For simplicity, taking the 4-6 SCMA as an example, (3) can be rewritten as:

$$I_{f_{n,k}\to v_{n,t}}(q_1) = \frac{1}{2\pi N_0}\cdot\exp(\frac{1}{2N_0 d_{n,k}(\boldsymbol{x})}) \cdot(I_{v_{n,r}\to f_{n,k}}(q_2)\cdot I_{v_{n,s}\to f_{n,k}}(q_3)), \tag{8}$$

where $q_i = 0, 1, \cdots, C-1$ (C is the size of constellation), the conventional 4-6 SCMA graph model is used; hence, the degree of FN is $d_f = 3$, r, s, t represents the edges connect to the kth FN in nth SSG, respectively. The messages pass from SVNs to FN in the probability domain is given by:

$$I_{v_{n,j}\to f_{n,t}}(q) = \alpha_{nor}\cdot I_{f_{n,s}\to v_{n,j}}(q) \cdot I_{Lv_{j,2n-1}\to v_{n,j}}(q)\cdot I_{Lv_{j,2n}\to v_{n,j}}(q), \tag{9}$$

where α_{nor} is the normalized factor; $q = 0, 1, \cdots, C-1$. Note that each SSG updates their SVNs simultaneously, as a result, each SVN delivers information to $\log_2 C$ corresponding LVNs after the update of SVN.

In the case when the NB-LDPC code is used, an SVN corresponds to only one LVN. Thus, the messages deliver from JVN to FN should be modified as:

$$I_{Jv_{n,j}\to f_{n,t}}(q) = \alpha_{nor}\cdot I_{f_{n,s}\to Jv_{n,j}}(q) \cdot\prod_{\forall p_{j,i}\in\psi^j_{Jv_{j,m}}} I_{p_{j,i}\to Jv_{j,m}}(q), \tag{10}$$

where $\psi^j_{Jv_{j,m}}$ is a check node set which includes all the CNs connect to $Jv_{j,m}$. It is obvious that the set $\psi^j_{Jv_{j,m}} = \psi^j_{Lv_{j,m}}$ when NB-LDPC code is applied to SG-JSG-SCMA. To make the algorithm more efficient and converge faster, a normalized factor α_{nor} should be added into (9) and (10).

b) LDPC VARIABLE NODES UPDATE

The update of LVN is similar to SVN, which is given by:

$$I_{p_{j,l}\to Lv_{j,m}} = I_{v_{\lceil\frac{m}{2}\rceil,j}\to Lv_{j,m}} + \sum_{\forall i\neq l: p_{j,i}\in\psi^j_{Jv_{j,m}}} I_{Lv_{j,m}\to p_{j,i}}. \tag{11}$$

The relationship that $\log_2 C$ LVNs correspond to one SVN is represented by the Gaussian rounding function $\lceil\cdot\rceil$, j denoted the jth LSG in SG-JSG. It should be noted that the number of users is equal to the number of LSG in SG-JSG.

4) MESSAGE EXCHANGE

The message exchange between SVN and LVN is the main reason for the performance gain achieved by the SG-JSG-SCMA. Therefore, it is treated as an independent part in this paper.

Essentially, the symbol-to-bit message transformation is a marginalization of the probability density function (PDF), and the calculation of $I_{Lv_{j,2n-1}\to v_{n,j}}(q)$ and $I_{Lv_{j,2n}\to v_{n,j}}(q)$ are its inverse transformation.

Firstly, we assume the mapping of symbol as $q = 0 \to 00$, $q = 1 \to 10, q = 2 \to 01, q = 3 \to 11$, which corresponds to the mapping over $GF(q)$. Taking the 4-point SCMA as an example, the marginalization of symbols' PDF can be written as:

$$\begin{aligned} I_{v_{n,k}\to Lv_{k,2n-1}}(0) &= \log\left(\frac{I_{v_{n,k}}(1) + I_{v_{n,k}}(3)}{I_{v_{n,k}}(0) + I_{v_{n,k}}(2)}\right) \\ I_{v_{n,k}\to Lv_{k,2n}}(1) &= \log\left(\frac{I_{v_{n,k}}(2) + I_{v_{n,k}}(3)}{I_{v_{n,k}}(0) + I_{v_{n,k}}(1)}\right). \end{aligned} \tag{12}$$

Note that $I_{v_{n,k}\to Lv_{k,2n-1}}$ and $I_{v_{n,k}\to Lv_{k,2n}}$ are messages that are delivered from SVN to LVNs, and the messages delivered in the opposite direction can be expressed as:

$$I_{Lv\to v_{n,j}}(q) = \begin{cases} (I_{Lv_{j,2n-1}}(b_1))\cdot(I_{Lv_{j,2n}}(b_2)), q = 0 \\ (I_{Lv_{j,2n-1}}(b_1))\cdot(1 - I_{Lv_{j,2n}}(b_2)), q = 1 \\ (1 - I_{Lv_{j,2n-1}}(b_1))\cdot(I_{Lv_{j,2n}}(b_2)), q = 2 \\ (1 - I_{Lv_{j,2n-1}}(b_1))\cdot(1 - I_{Lv_{j,2n}}(b_2)), q = 3, \end{cases} \tag{13}$$

where $b_1 = b_2 = 0$, $I_{Lv_{j,2n-1}}$ and $I_{Lv_{j,2n}}$ are defined by:

$$I_{Lv_{j,2n-1}} = \frac{\exp\left(\sum_{\forall l:p_{j,l}\in\psi^{j}_{Lv_{j,2n-1}}} I_{p_{j,l}\to Lv_{j,2n-1}}\right)}{1+\exp\left(\sum_{\forall l:p_{j,l}\in\psi^{j}_{Lv_{j,2n-1}}} I_{p_{j,l}\to Lv_{j,2n-1}}\right)}, \quad (14)$$

and

$$I_{Lv_{j,2n}} = \frac{\exp\left(\sum_{\forall l:p_{j,l}\in\psi^{j}_{Lv_{j,2n}}} I_{p_{j,l}\to Lv_{j,2n}}\right)}{1+\exp\left(\sum_{\forall l:p_{j,l}\in\psi^{j}_{Lv_{j,2n}}} I_{p_{j,l}\to Lv_{j,2n}}\right)}. \quad (15)$$

To make the modified MPA easy to follow, a partial view of message flow in B-LDPC coded SG-JSG-SCMA is depicted in Fig. 4. As can be seen from the figure, according to the MPA, the messages represented by dash lines are generated by the messages which are denoted by solid lines, and vice versa.

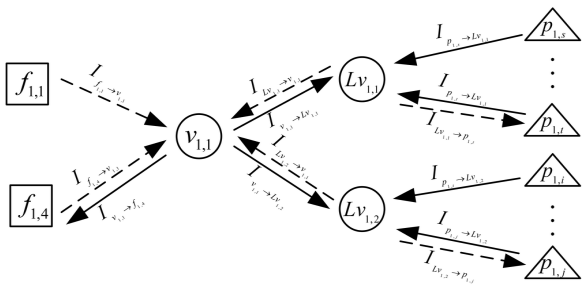

FIGURE 4. Partial view of message flow in B-LDPC coded SG-JSG-SCMA.

B. MODIFIED MPA IN NB-LDPC CODED SG-JSG-SCMA

1) FUNCTION NODES UPDATE

As for NB-LDPC coded SG-JSG-SCMA, the update of FN is completely the same as the B-LDPC coded one.

2) CHECK NODES UPDATE

For the CN update in NB-LDPC coded SG-JSG, we adopt FFT-BP [28] as the decoding algorithm in this paper. Therefore, the CN update is given as:

$$I_{p_{k,l}\to Jv_{k,i}} = \mathcal{F}\left(\prod_{\forall m\neq i:Jv_m\in\phi^{j}_{l}} \mathcal{F}(I_{Jv_{k,m}\to p_{k,l}})\right), \quad (16)$$

where $\mathcal{F}$ is the Fourier transformation over $GF(q)$. It should be noted that FFT-BP is a symbol-level MPA, and the dimension of input messages are the same as that of SVN.

3) JOINT VARIABLE NODES UPDATE

When FFT-BP algorithm is applied, the update of JVN is:

$$I_{p_{j,l}\to Jv_{j,m}}(q) = I_{f_{n,k}\to Jv_{n,t}}(q)\cdot I_{f_{n,k}\to Jv_{n,s}}(q) \cdot \prod_{\forall i\neq l:p_{j,i}\in\psi^{j}_{Jv_{j,m}}} I_{Jv_{j,m}\to p_{j,i}}(q). \quad (17)$$

Note that the messages in (17) are defined over the probability domain. An important observation from (17) is that the SVN and LVN are merged into a JVN, which indicates that the message vectors deliver to the JVN from the left and right side of SG-JSG have the same dimension. Therefore, the NB-LDPC codes that are defined over $GF(4)$ and $GF(16)$ can be applied in this paper.

As shown in Fig. 5, the process of JVN update is presented in a straightforward manner. It can be observed that the extrinsic messages, which is denoted by dash lines, flow from JVN into FN, and are generated by messages sent from connected CNs along with the intrinsic messages. Similarly, the incoming extrinsic messages of CNs include the information coming from FNs.

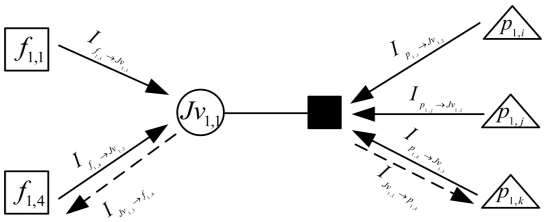

FIGURE 5. Partial view of JVN update in NB-LDPC coded SG-JSG-SCMA.

It should be noted that in NB-LDPC coded SG-JSG-SCMA, the SVN and LVN can be directly linked without connected model, as a result, the message exchange between SVNs and LVNs is not necessary in NB-LDPC coded SG-JSG-SCMA. However, due to the complexity of SCMA detection and NB-LDPC code decoding are dominated by $O(q^{d_f})$ and $O(q^2)$ [29], respectively. The computational complexity is very high with straightforward implementation of MPA and FFT-BP on NB-LDPC coded SG-JSG-SCMA. To render the system affordable for practical implementation, a simplified joint detection and decoding algorithm is proposed in the sequel.

IV. SIMPLIFIED ALGORITHM FOR A NB-LDPC CODED SG-JSG-SCMA SYSTEM

In this section, a reduced complexity algorithm for the SG-JSG-SCMA system is introduced, along with a JTR that can represent the search space of NB-LDPC coded SG-JSG-SCMA.

A. JOINT TRELLIS REPRESENTATION FOR SG-JSG-SCMA

We define a mapping between constellation point and $GF(q)$; hence, the constellation points in SCMA correspond to the

elements over $GF(q)$, which can be represented as:

$$f : constellation \rightarrow GF(q). \tag{18}$$

Moreover, NB-LDPC codes are defined over $GF(q)$, and can be represented by trellis [30]. As can be seen from (18) and (4), the detection process of SCMA can also be represented by trellis. Note that the trellis used in this paper is not the same as the ones used for convolutional codes or of Markovian state spaces. It represents the different Galois field values that the symbols participating in the FN and CN update can take. Inspired by these ideas, we propose a JTR which can depict the message flow and search space in NB-LDPC coded SG-JSG-SCMA.

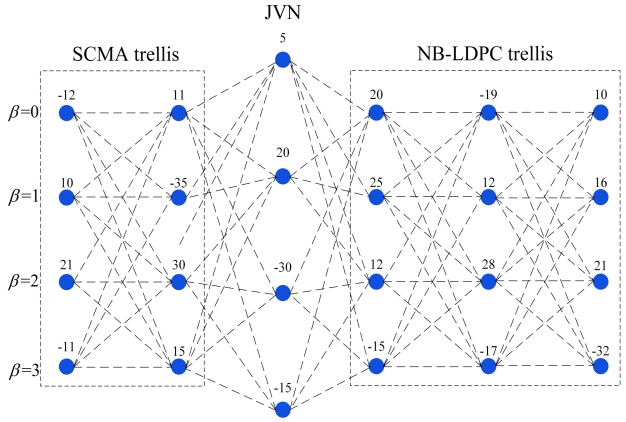

FIGURE 6. Joint trellis representation of NB-LDPC coded SG-JSG-SCMA with $d_f = 3, d_p = 4$.

Fig. 6 depicts the JTR in a NB-LDPC coded SG-JSG-SCMA system. As shown in the figure, there are two separate trellises that are linked by the JVN; hence, JVN belongs to both SCMA trellis and LDPC trellis. For the SCMA trellis in JTR, the vertexes in trellis represent the constellation points which can be mapped to $GF(q)$, thus, the number of rows in the left side trellis equals to the size of constellation C. It should be noted that each vertex corresponds to a complex SCMA codewords in a codebook. The dash lines in trellis between different columns are all possible paths that have to be searched when calculating $d_{n,k}$ in (4), and the real numbers above vertexes are normalized logarithm domain messages of each constellation point. The trellis at the right side represents the search space of CN update in NB-LDPC codes, each row represents the possible symbol values over $GF(4)$. In the NB-LDPC trellis, the dash paths connect the incoming message vectors and form all possible codewords when decoding. For the JTR, two trellises are linked by a JVN, which is represented by four vertexes on the JTR in the figure. This follows from the fact that each JVN carries a C dimension message vector in a C point SCMA system. It is clear that the JTR denotes the messages delivered to JVN in one iteration. Each dash line that starts from SCMA trellis and ends at NB-LDPC trellis represents a possible case to calculate messages deliver from CN and FN to JVN.

Basically, the effect of JTR is to change the search space, which represents by a set typically, into vertexes and paths; hence, the complexity reduction in SG-JSG-SCMA comes from elimination of paths in the JTR.

In the JTR, all the possible cases that should be calculated to obtain the messages flow into JVN can be represented as:

$$\begin{aligned}\chi_S(q) = \{\boldsymbol{x_k} = [x_1^{k_1}[\beta], \cdots, x_{d_f}^{k_{d_f}}[\beta]] : \\ \forall \boldsymbol{k} = [k_1, \cdots, k_{d_f}] \in \{1, \cdots, q\}^{d_f}\},\end{aligned} \tag{19}$$

and

$$\begin{aligned}\chi_L(q) = \{\boldsymbol{c_k} = [c_1^{k_1}[\beta], \cdots, c_{d_p}^{k_{d_p}}[\beta]] : \\ \forall \boldsymbol{k} = [k_1, \cdots, k_{d_p}] \in \{1, \cdots, q\}^{d_p}\}.\end{aligned} \tag{20}$$

Clearly, the cardinality of (19) and (20) can be written as:

$$|\chi_S(q)| = q^{d_f}, \tag{21}$$

and

$$|\chi_L(q)| = q^{d_p}. \tag{22}$$

It is clear that the cardinality in (21) and (22) are important parameters that can reflect the computational complexity of SG-JSG-SCMA; hence, a way to reduce the complexity of NB-LDPC coded SG-JSG-SCMA is to find proper subsets of $\chi_S(q)$ and $\chi_L(q)$ to process joint detection and decoding with margin performance loss.

B. JOINT TRELLIS BASED JOINT DECODING AND DETECTION ALGORITHM

Based on the JTR, we propose a novel simplified JTDD algorithm for NB-LDPC coded SG-JSG-SCMA to reduce the computational complexity. According to the JTR, a simple way to reduce the complexity of NB-LDPC coded SG-JSG is to eliminate the paths that make little contribution to the FN and CN update. As noted in [29] and [30], the paths that consist of symbols with high reliability in NB-LDPC codes dominate their error rate performance. On the other hand, an edge selection based detector by using Gaussian forcing is reported in [31] to reduce the detection complexity in LDS-OFDM system. Therefore, d_f in (21) can be reduced by selecting proper columns in the JTR to involve in joint detection and decoding. As such, only partial messages are utilized to process MPA on the SG-JSG.

Fig. 7 shows the JTR of proposed JTDD in each iteration. In the figure, the dash paths in the figure are all the possible cases to calculate messages delivered from CN and FN to JVN. The solid paths represent the actual cases that have to be calculated after eliminating a column in the SCMA trellis to reduce the effective d_f in (21) and selecting n_m most reliable symbols in the NB-LDPC trellis to reduce the dimension of message vectors q in (22).

In a SCMA system, it can be inferred that the better channel quality, the higher reliability to pass message through this channel; hence, we can use the channel quality as the criteria for proper column selection. Each column of SCMA trellis in

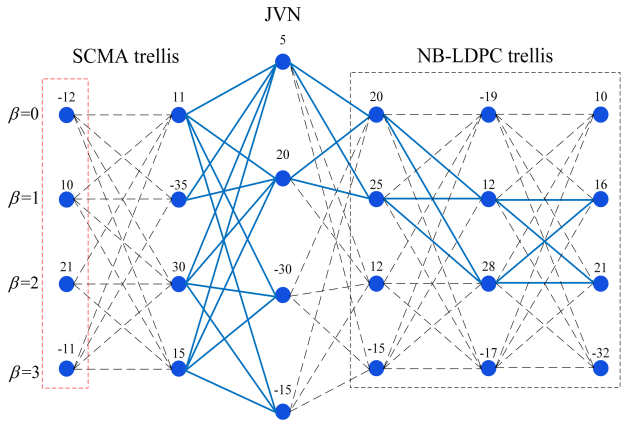

FIGURE 7. Simplified joint trellis representation of NB-LDPC coded SG-JSG-SCMA with $d_f = 3, d_p = 4$.

JTR corresponds to a different $h_{j,k}$ ($j = 1, \cdots, d_f$). To make such a column selection scheme more efficient, the messages at the eliminated columns are utilized as a compensation term in the FN update. As such, (4) can be decomposed as:

$$d_{n,k}(\boldsymbol{x}) = \frac{1}{\sigma^2}\|y_{n,k} - h_{j,k}x_{j,k} - \sum_{i\in\xi^n_{k,Sel}} h_{i,k}x_{i,k} - \sum_{t\neq j, t\notin\xi^n_{k,Sel}} h_{t,k}x_{t,k}\|, \quad (23)$$

where $\xi^n_{k,Sel}$ is a set that contains all the selected columns in the kth JTR of nth SSG. The last term in (23) denotes the eliminated columns, which can be modeled as a Gaussian random variable (RV) that follows the distribution $\mathcal{CN}(\mu^{(n)}_{j,k}, (\sigma^{(n)}_{j,k})^2)$ as the modulus of $\|h_{t,k}\|$ is relatively small.

As noted in [32], the means $\mu^{(n)}_{j,k}$ can converge to the correct values as the MPA proceeds on a Gaussian graphical models. Therefore, the means should be updated at the current iteration as the feedback information for the next iteration. On the other hand, we find out that it is more efficient if the variances $(\sigma^{(n)}_{j,k})^2$ can be updated like $\mu^{(n)}_{j,k}$. Consequently, the update of $\mu^{(n)}_{j,k}$ and $(\sigma^{(n)}_{j,k})^2$ can be written as:

$$\mu^{(n)}_{j,k} = \sum_{t\neq j, t\notin\xi^n_{k,Sel}} h_{t,k}\cdot\mathbb{E}[x_{t,k}], \quad (24)$$

and

$$(\sigma^{(n)}_{j,k})^2 = \sum_{t\neq j, t\notin\xi^n_{k,Sel}} |h_{t,k}|^2\cdot\mathrm{Var}(x_{t,k}) + \sigma^2, \quad (25)$$

where $\mathbb{E}[\cdot]$ and $\mathrm{Var}(\cdot)$ are the mathematical expectation and variances, respectively, which can be further represented as:

$$\mathbb{E}[x_{t,k}] = \sum_{q\in GF(q)} I_{v_{n,t}\to c_{n,k}}(q)\cdot x_{t,k}, \quad (26)$$

and

$$\mathrm{Var}(x_{t,k}) = \sum_{q\in GF(q)} I_{v_{n,t}\to c_{n,k}}(q)\cdot|x_{t,k}|^2 - \mathbb{E}[x_{t,k}]^2. \quad (27)$$

Based on the compensation term in (24) and (25) that uses Gaussian forcing and information feedback strategy, (23) can be rewritten as:

$$d_{n,k}(\boldsymbol{x}) = \frac{1}{(\sigma^{(n)}_{j,k})^2}\|y_{n,k} - h_{j,k}x_{j,k} - \sum_{i\in\xi^n_{k,Sel}} h_{i,k}x_{i,k} - \mu^{(n)}_{j,k}\|. \quad (28)$$

According to (28), only the selected columns with high channel quality, i.e., the modulus of $h_{j,k}$ that is sufficiently will be involved in the joint detection and decoding process. Therefore, the cardinality of $\chi_S(q)$ reduces from q^{d_f} to $q^{d_{f,Sel}}$ ($d_{f,Sel} < d_f$). Such an columns selection strategy with Gaussian forcing and information feedback is not efficient in an individual NB-LDPC coded SCMA receiver as the messages in a disjoint receiver only deliver in a single direction. However, the error rate performance can be enhanced in a SG-JSG-SCMA system, as will be evidenced later.[2]

After the messages flowing from the SCMA trellis to the NB-LDPC trellis in JTR, the computational complexity can be further reduced by only selecting n_m most reliable symbols in each column to construct the paths that follow the parity-check equations; hence, (20) can be modified as:

$$\chi_L(n_m) = \{\boldsymbol{c_k} = [c^{k_1}_1[\beta], \cdots, c^{k_{d_p}}_{d_p}[\beta]] : \forall \boldsymbol{k} = [k_1, \cdots, k_{d_p}] \in \{1, \cdots, n_m\}^{d_p}\}. \quad (29)$$

As noted in [29], a deviated subset $\chi_L(n_m, n_c)$, which can achieve comparable error rate performance as original $\chi_L(n_m)$, is defined as:

$$\chi_L(n_m, n_c) = \chi_L(n_m)^{(0)} \bigcup \chi_L(n_m)^{(1)} \bigcup \cdots \bigcup \chi_L(n_m)^{(n_c)}, \quad (30)$$

where $n_c \leq d_p - 1$, $\chi_L(n_m)^{(p)}$ is the subset of $\chi_L(n_m)$ that differs from the most reliable combination in p entries. Hence, the cardinality of $\chi_L(n_m, n_c)$ is given by:

$$|\chi_L(n_m, n_c)| = \sum_{k=0}^{n_c}\binom{d_p-1}{k}(n_m-1)^k \approx \sum_{k=0}^{n_c}\binom{d_p-1}{k}(n_m)^{n_c}. \quad (31)$$

It should be noted that the approximation in (31) is obtained by applying Taylor series expansion, and truncating those negligible terms. To compensate the possible performance loss caused by only selecting n_m most reliable symbols at each column in the JTR, the CN update in JTDD can be rewritten as:

$$I_{p_{j,l}\to Jv_{j,m}} = I_{p_{j,l}\to Jv_{j,m}} + \sum_{\forall \boldsymbol{c_k}\in\chi_L(n_m,n_c)} I_{Jv_{j,m}\to p_{j,i}}(\boldsymbol{c_k}), \quad (32)$$

where

$$I_{Jv_{j,m}\to p_{j,i}}(\boldsymbol{c_k}) = \max(I_{Jv_{j,m}\to p_{j,i}}(\boldsymbol{c_k}) - \alpha_{off}, 0), \quad \text{if} \quad I_{Jv_{j,m}\to p_{j,i}}(\boldsymbol{c_k}) > 0, \quad (33)$$

[2]It should be noted that the performance of using only partial messages in a disjoint and Turbo structured receiver is not as efficient as the SG-JSG-SCMA, which indicates that the performance loss is quite significant. In this paper, we merely show the result of JTDD to illustrate its effectiveness.

and

$$I_{J v_{j,m} \to p_{j,i}}(\boldsymbol{c_k}) = \min(I_{J v_{j,m} \to p_{j,i}}(\boldsymbol{c_k}) - \alpha_{off}, 0), \quad \text{if} \quad I_{J v_{j,m} \to p_{j,i}}(\boldsymbol{c_k}) < 0. \tag{34}$$

Note that α_{off} is a parameter which can be determined through density evolution [33], [34]. By introducing such an offset into the update of CN when only n_m dimension messages are used, the performance can be improved.

V. SIMULATION RESULTS AND DISCUSSION

In this section, the simulation results of SG-JSG-SCMA, along with the analysis and discussion, are presented.

A. BER COMPARISON

In this paper, the error rate performances of SG-JSG-SCMA systems are presented. The indicator matrix in (1) (including parameters $K = 4; J = 6; d_f = 3; d_u = 2; \lambda = 150\%$) and $\boldsymbol{F_{8\times 16}}$ in (35), as shown at the bottom of this page, (including parameters $K = 8; J = 16; d_f = 4; d_u = 2; \lambda = 200\%$) are evaluated over the 3 taps SUI-3, 4-taps ITU-Pedestrian channel-A and 6-taps ITU-Pedestrian channel-B. To ensure well performance of our scheme can be achieved under mobility conditions, 6 taps ITU-Vehicular channel model is also simulated, the codebook with size $C = 4$ and $C = 16$ are utilized for the simulations. The codebook is designed according to [8]. For the disjoint receiver, the maximum iteration number of SCMA detector and LDPC decoder are 6 and 20, respectively. The maximum iterative times of SG-JSG-SCMA are all set to 10 in simulations. Considering the requirements of power consumption and latency in mMTC, LDPC code with code length equals to 256 and 1008 are simulated in this paper to illustrate the effectiveness of the proposed scheme. Note that the B-LDPC and NB-LDPC codes used in this paper were constructed in [29], [35], and [36], respectively, which have been proved to be well-performed.

Fig. 8 shows the performance comparison of the SG-JSG-SCMA receiver, Turbo-style receivers with different outer and inner iterations and the individual receiver. It can be seen that SG-JSG-SCMA brings about 4.5dB performance gain compare to individual receiver. Furthermore, SG-JSG-SCMA achieves a better performance than the

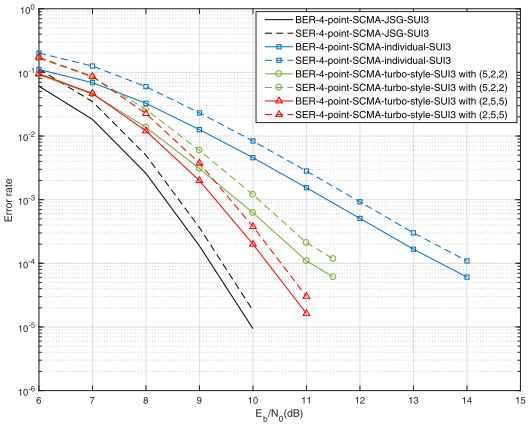

FIGURE 8. Performance comparisons of different types of B-LDPC coded 4-point SCMA receivers with code length $N = 256$ and code rate $r = 0.5$.

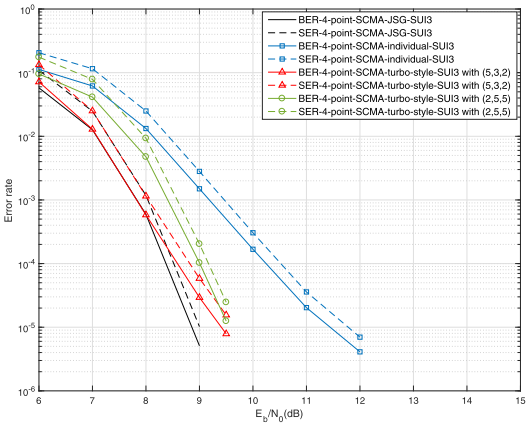

FIGURE 9. Performance comparisons of different types of B-LDPC coded 4-point SCMA receivers with code length $N = 1008$ and code rate $r = 0.5$.

Turbo-style receiver[3] with 1-1.5dB gain at BER= $10^{-4.3}$ under the condition of comparable computational complexity. It should be noted that the SG-JSG-SCMA can also achieve a better symbol error rate (SER) performance compared to the other two types of receivers. Fig. 9 indicates that the SG-JSG-SCMA is also suitable with a moderate length B-LDPC code. As depicted in the figure, in comparison to the individual receiver, the SG-JSG-SCMA achieves nearly

[3]For brevity, we use $(I_{out}, I_{ldpc}, I_{scma})$ to denote the outer and inner iterations of Turbo-style receiver used in the simulation in the following.

$$\boldsymbol{F}_{8\times 16} = \begin{bmatrix} 0 & 0 & 0 & 1 & 0 & 0 & 0 & 1 & 0 & 0 & 0 & 1 & 0 & 1 & 0 & 0 \\ 1 & 0 & 0 & 0 & 0 & 1 & 0 & 0 & 0 & 1 & 0 & 0 & 0 & 0 & 0 & 1 \\ 0 & 0 & 1 & 0 & 1 & 0 & 0 & 0 & 0 & 0 & 1 & 0 & 0 & 1 & 0 & 0 \\ 0 & 1 & 0 & 0 & 0 & 0 & 0 & 1 & 0 & 0 & 0 & 0 & 1 & 0 & 0 & 1 \\ 0 & 0 & 0 & 1 & 0 & 0 & 1 & 0 & 1 & 0 & 0 & 0 & 0 & 0 & 1 & 0 \\ 0 & 0 & 1 & 0 & 0 & 1 & 0 & 0 & 0 & 0 & 1 & 0 & 1 & 0 & 0 & 0 \\ 1 & 0 & 0 & 0 & 1 & 0 & 0 & 0 & 1 & 0 & 0 & 1 & 0 & 0 & 0 & 0 \\ 0 & 1 & 0 & 0 & 0 & 0 & 1 & 0 & 0 & 1 & 0 & 0 & 0 & 0 & 1 & 0 \end{bmatrix}. \tag{35}$$

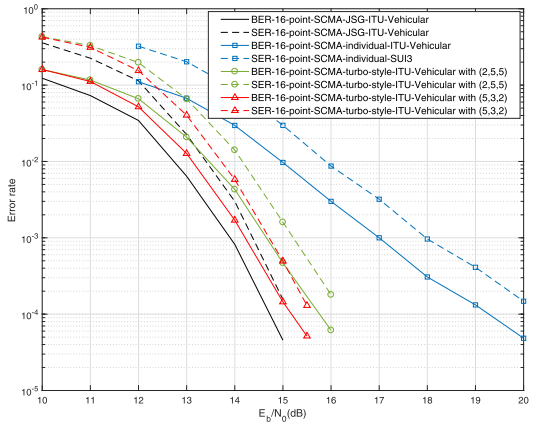

FIGURE 10. Performance comparisons of different types of B-LDPC coded 16-point SCMA receivers with code length $N = 256$ and code rate $r = 0.5$.

3dB performance gain at both BER and SER equal to 10^{-5}. Moreover, the SG-JSG-SCMA brings about 0.5dB performance gain at BER $= 10^{-5}$ compared to the Turbo-structured receiver when the computational complexity is comparable. It can be also inferred from Fig. 8 and Fig. 9 that the performance gain of SG-JSG-SCMA shrinks as the code length increases, i.e., the performance of SG-JSG-SCMA is highly relative to the error correction ability of LDPC codes.

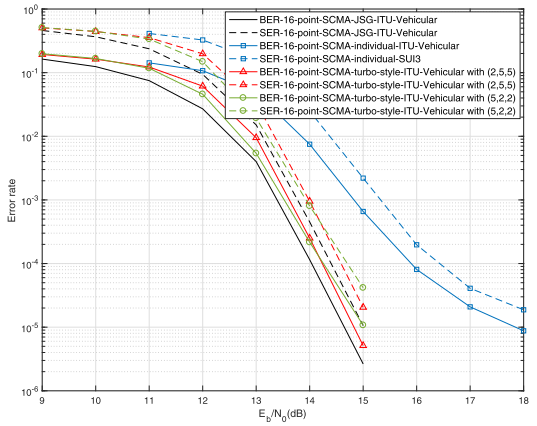

FIGURE 11. Performance comparisons of different types of B-LDPC coded 16-point SCMA receivers with code length $N = 1008$ and code rate $r = 0.5$.

We also investigate the performance of 16-point B-LDPC coded SG-JSG-SCMA over 6 taps ITU-Vehicular channel model with different code length in Fig. 10 and Fig. 11. As can be seen from the figure, the SG-JSG-SCMA structure performs well with constellation size C equals to 16. The 16-point SG-JSG-SCMA achieves 4.2dB and 3.6dB gain in comparison to disjoint receiver at BER$= 10^{-4}$ with code length $N = 256$ and $N = 1008$, respectively. Additionally, the 16-point SG-JSG-SCMA also outperforms the Turbo-style receiver with approximately 0.5-1.2dB and 0.2-0.5dB gain at BER$= 10^{-4.6}$ with code length equal to 256 and 1008, respectively. It should be also noted that the performance of SER in 16-point SCMA system is inferior to 4-point SCMA system, which indicates that the gap between the curves of BER and SER is larger. This follows from the fact that there are more data in a block for a 16-point SCMA system; hence, it is more likely to appear errors in a data block. However, as shown in the figure, the gap between SER and BER shrinks in the high SNR region, i.e., the joint structure is able to improve the performance of SER of 16-point SCMA, which is meaningful to the practical implementation of SG-JSG-SCMA.

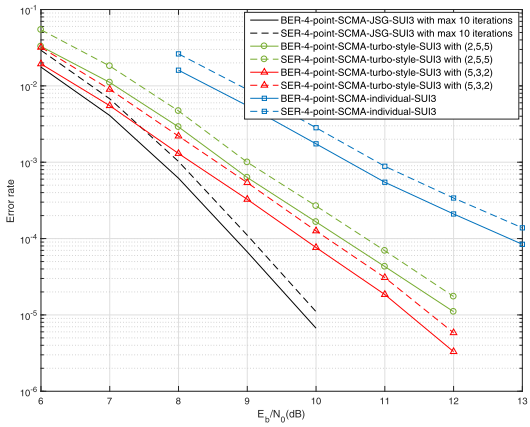

FIGURE 12. Performance comparisons of different types of NB-LDPC coded 4-point SCMA receivers with code length $N = 260$ and code rate $r = 0.5$.

The performances of NB-LDPC coded SG-JSG-SCMA system are evaluated in Fig. 12 and Fig. 13. As shown in the figures, both NB-LDPC coded 4-point and 16-point SG-JSG-SCMA outperform other receiver types. Compared with the individual receiver, SG-JSG-SCMA defined over $GF(4)$ can obtain about 2.5-3dB gain in the medium to high SNR region. Moreover, NB-LDPC coded 4-point SG-JSG-SCMA brings about 1.5-2dB performance gain at BER equal to 10^{-5} compared to Turbo structured SG-JSG-SCMA with different outer and inner iterations. In addition, the performance gap between NB-LDPC coded 16-point SG-JSG-SCMA and individual receiver is approximately 2.8dB at BER$= 10^{-4}$. In contrast to the Turbo structured receiver, SG-JSG-SCMA obtains about 0.6-1dB gain in the medium to high SNR region.

The performance of SG-JSG-SCMA by using JTDD with loads of 150% and 200% over 6 taps ITU-Vehicular channel are also evaluated and shown in Fig. 14. To make a better trade-off between complexity and error rate performance, $d_f - 1$ edges, $n_m = 2$ symbols ($n_c = 1$) and $\alpha_{off} = 0.6$ are chosen as the parameters in the JTDD. As shown in the figure, JTDD is capable of achieving an error rate performance within 0.5dB and 0.8dB from the original NB-LDPC coded SG-JSG-SCMA for 150% and 200% overloading systems, respectively, which can be attributed to the sufficient messages exchange between SSGs and NB-LSGs, i.e., the significant performance loss caused by only using partial messages can be compensated as the messages are

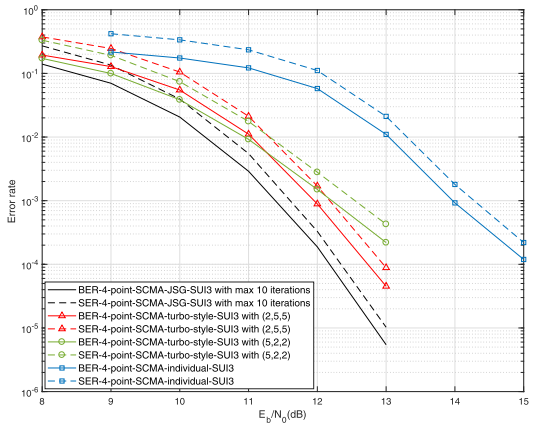

FIGURE 13. Performance comparisons of different types of NB-LDPC coded 16-point SCMA receivers with code length $N = 260$ and code rate $r = 0.5$.

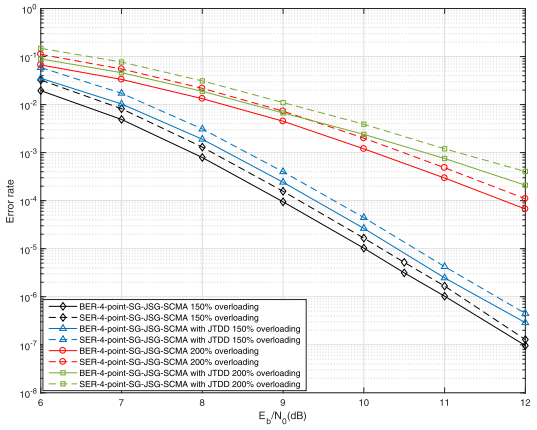

FIGURE 14. Performance comparisons of different algorithms for NB-LDPC coded SG-JSG-SCMA.

fully exchanged between the SCMA detector and NB-LDPC decoder. However, due to the loss of passing messages, the convergence behavior of JTDD is affected, more explicitly, JTDD needs another two more iterations to converge. Nonetheless, the complexity of JTDD is still much lower than the original algorithm, and the performance loss is acceptable. According to the results shown in Fig. 8-Fig. 14, it can be inferred that both B-LDPC and NB-LDPC coded SG-JSG-SCMA is suitable for different channel conditions.

The key of the SG-JSG-SCMA is to change the interference pattern being seen by each user, and limit the amount of interference incurred on each OFDMA subcarrier. It should be mentioned that the performance gain achieved by SG-JSG-SCMA comes from adequate message exchange and information feedback strategy. As shown in Sec. III, the messages over edges exchange between LSGs and SSGs at each iteration, indicates that the update of FNs and CNs receive the information from LSGs and SSGs, respectively, to update their messages. The other reason for the superiority of the SG-JSG-SCMA is the commonality of LDPC decoder and SCMA detector, i.e., the sparse graph model and MPA. This makes the message over SG-JSG more reliable and can be directly used with simple normalization. As pointed out by [15], [16], [33], [34], [37], and [38], the convergence behavior of SG-JSG-SCMA can be analyzed by extrinsic information transition (EXIT) chart or density evolution (DE), which are widely utilized on the iterative system.

B. ANALYSIS AND DISCUSSION

1) MULTI-PATH DIVERSITY

From Fig. 15, we can observe that the BER performance of ITU-Pedestrian channel-A is inferior to that of ITU-Pedestrian channel-B, indicating that the multi-path diversity is exploited by the SG-JSG-SCMA system under different overloading conditions, which can be attributed to the fact that ITU-Pedestrian channel-B has 6 paths while ITU-Pedestrian channel-A has 4 paths. However, the multi-path diversity gain achieved by SG-JSG-SCMA is not very significant especially in the region of low E_b/N_0. Furthermore, as can be seen from the figure, the NB-LDPC coded SG-JSG-SCMA using JTDD can also exploit the multi-path diversity over different channel models; hence, SG-JSG-SCMA with JTDD enjoys the multi-path diversity gain like the original algorithm, which illustrates the validity of JTDD. It should be noted that the multi-path diversity can be maximized by applying other techniques to SG-JSG-SCMA system if necessary [39], [40].

2) PROCESSING LATENCY

In some delay-sensitive mMTC applications, latency is an important performance metric. Hence, it would be of interest to show the processing latency of the proposed SG-JSG-SCMA. In this paper, we simply use the simulation execution time as the measurement of processing latency, which was presented in [41] and [42]. To eliminate the influence caused by devices and software, we set the execution

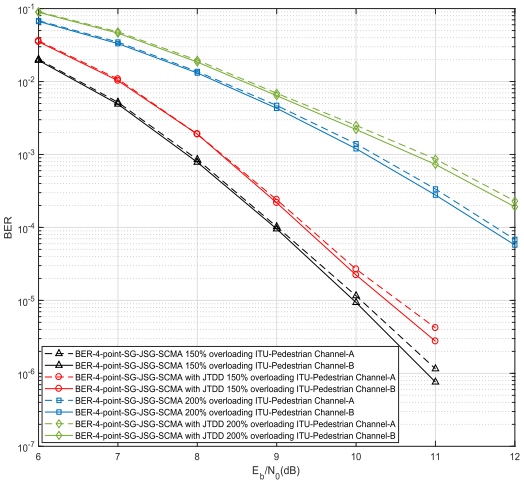

FIGURE 15. Performance of SG-JSG-SCMA over different multi-path channels under different overloading conditions.

TABLE 2. Latency comparison of different types of receivers.

	Individual	Turbo-style with (5,2,2)	Turbo-style with (2,5,5)	SG-JSG-SCMA
$C = 4, N = 256$ B-LDPC	1.0000	1.0221	1.0533	1.0066
$C = 4, N = 1008$ B-LDPC	1.0000	1.6199	1.7573	1.4907
$C = 16, N = 256$ B-LDPC	1.0000	1.6171	1.6886	1.8350
$C = 16, N = 1008$ B-LDPC	1.0000	1.7236	1.8150	1.8880
$C = 4, N = 260$ NB-LDPC	1.0000	1.4672	1.5937	1.4650
$C = 4, N = 260$ with JTDD	/	/	/	0.9657
$C = 16, N = 260$ NB-LDPC	1.0000	3.0660	3.2876	1.7633

time of individual receiver as baseline and normalize it to unity. Consequently, we can define a parameter that can reflect the relative latency of different types of receiver, i.e.,

$$L = \frac{T_{oth}}{T_{ind}}, \tag{36}$$

where T_{ind} and T_{oth} are the simulation execution time of individual receiver and other types of receivers, respectively. The processing latency of three different types of receivers are summarized in Table 2. Note that the execution time is calculated by averaging the total time of Monte-Carlo simulation.

As shown in the table, the latency of 4-point SG-JSG-SCMA receivers are all shorter than Turbo-style receivers with different inner and outer iterations, which follows from the fact that only outer iterations are necessary in SG-JSG-SCMA. However, the latency of B-LDPC coded 16-point SG-JSG-SCMA receivers are all longer than Turbo-style receivers. This is related to the fact that the marginalization and its inverse transformation are needed in each iteration, which involve additional calculations for a B-LDPC coded 16-point SG-JSG-SCMA system. However, for the NB-LDPC coded 16-point SG-JSG-SCMA, the LVN and SVN are merged into JVN; hence, the messages can be directly exchanged between NB-LSGs and SSGs without extra transformations, this is the main reason for latency reduction in the NB-LDPC coded 16-point SG-JSG-SCMA. It is worth mentioning that the latency of the proposed JTDD is even lower than the individual receiver, which indicates the efficiency of our scheme.

3) NEAR-FAR EFFECT

Fig. 16 shows the performance of near-far resistance for SG-JSG-SCMA with different structures over the 6 taps ITU-Vehicular Channel. The simulation is carried out for the case when $E_b/N_0 = 10$ dB for the first user, and E_b/N_0 of other users are different. The BER of the first user is plotted against $\Delta E_b/N_0$ which represents the difference in E_b/N_0 between the user of interest and the other users. More explicitly, when the first users SNR $E_b/N_0 = 10$ dB, the other users SNR equals to $\Delta E_b/N_0$ plus 10 dB. It can be observed that unequal received power has a minor effect on the performance of user of interest for different types of SG-JSG-SCMA receiver. Both 4-point B-LDPC coded and NB-LDPC coded SG-JSG-SCMA systems exhibit certain robustness against unequal received power as the iterative processing, i.e., the near-far effect can be alleviated by the low density spreading techniques and effective MPA. From the simulation result, it should be also noted that the NB-LDPC coded SG-JSG-SCMA is more robust to the near-far effect than B-LDPC coded SG-JSG-SCMA.

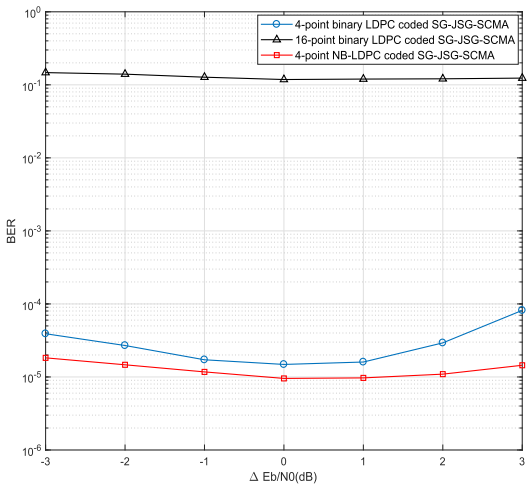

FIGURE 16. Near-far effect of SG-JSG-SCMA.

4) COMPLEXITY ANALYSIS

In this part of analysis, we mainly focus on the complexity of JTDD based SG-JSG-SCMA, which can significantly reduce the complexity of the original NB-LDPC coded SG-JSG-SCMA. As the same B-LDPC or NB-LDPC code is applied to all the investigated receivers, the complexity of the receiver mainly depends on the number of required iterations and the search space in each iteration. As defined in (19) and (20), the search space of SG-JSG-SCMA can be estimated by (21) and (22), i.e., the total search space for a SG-JSG-SCMA system at each iteration is given by:

$$|\chi_T| = |\chi_S| + |\chi_L|. \tag{37}$$

Fig. 17 depicts the total search space of different SG-JSG-SCMA for a frame of data (the length of a frame equals to the code length N in this paper). In Fig. 17, the search space of different algorithms for NB-LDPC coded SG-JSG-SCMA is investigated. As shown in the figure,

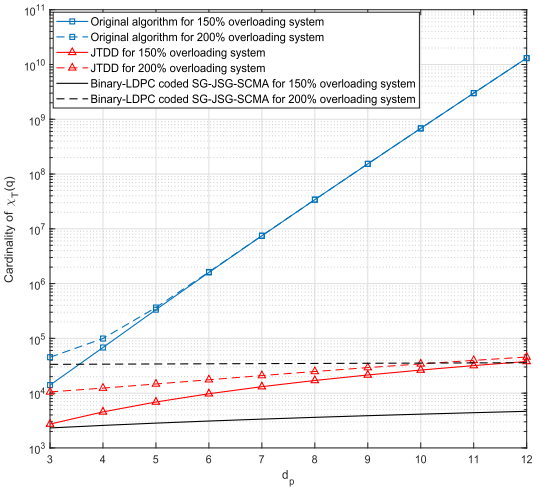

FIGURE 17. Comparison of $|\chi_T|$ over different overloading SG-JSG-SCMA system.

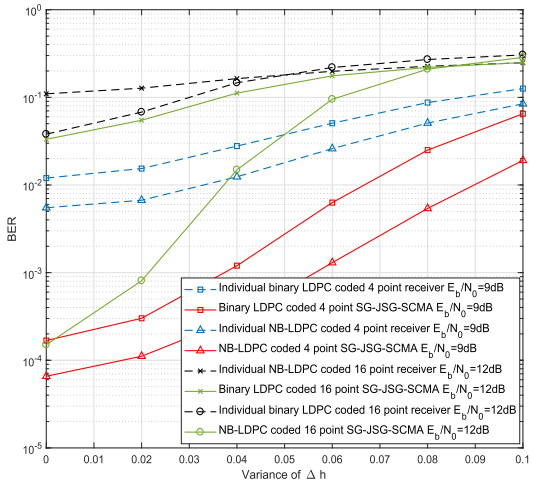

FIGURE 18. The effects of the channel estimation error on the BER performance for different types of receiver.

$|\chi_T|$ of SG-JSG-SCMA with JTDD is far lower than $|\chi_T|$ of original SG-JSG-SCMA, especially when the d_p is large. Another observation is that the search space of JTDD based NB-LDPC coded SG-JSG-SCMA system with 200% overloading is even smaller than the original B-LDPC coded SG-JSG-SCMA with 200% overloading when $d_p < 10$. This follows from the fact that JTDD reduces the search space of both LSGs and SSGs. Therefore, the total search space of JTDD based SG-JSG-SCMA can be reduced significantly. As noted in [14], [31], and [43], more columns can be eliminated from the joint trellis when d_f is larger, i.e., fewer columns in the JTR are required to deliver messages; hence, the search space can be further reduced with negligible performance loss in a SG-JSG-SCMA system if the d_f of SSG is large.

5) EFFECT OF CHANNEL ESTIMATION ERROR

As the channel state information (CSI) of each user should be estimated to detect the transmitted information, and the estimation error of CSI cannot be avoided in a practical system. It is necessary to investigate the robustness of our proposed SG-JSG-SCMA against the estimation error of CSI. The estimated error of channel can be modeled as:

$$\hat{h} = h + \Delta h, \tag{38}$$

where $\hat{h}$ and h are the estimated CSI and actual CSI, respectively. Δh denotes the error of the CSI estimation, which can be modeled as a random variable that follows the complex Gaussian distribution $\mathcal{CN}(0, \sigma^2)$ according to [9]. We adopt 3 taps SUI-3 as the channel model, $E_b/N_0 = 9$ dB for 4-point and $E_b/N_0 = 12$ dB for 16-point SG-JSG-SCMA. It should be noted that the variance of $\hat{h}$ is normalized to unity in our simulations.

An important observation from Fig. 18 is that 4-point SG-JSG-SCMA is far more sensitive to the CSI estimation error than the individual receiver, i.e., the slope of the 4-point SG-JSG-SCMA curves are larger than the individual ones.

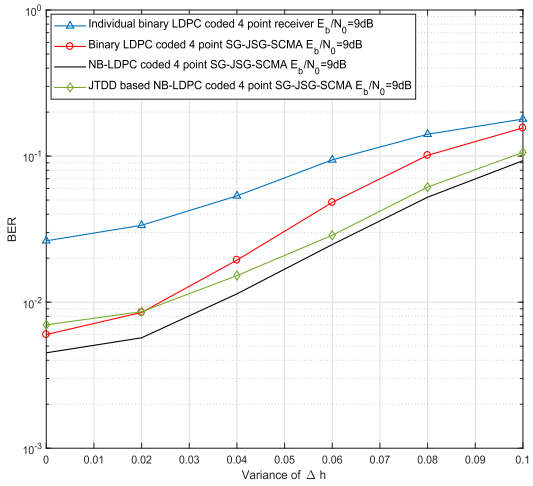

FIGURE 19. The effects of the channel estimation error on the BER performance for JTDD algorithm under 200% overloading.

However, there is a gap between these two types of receivers, which gradually shrinks as Δh increases. This is related to the different BER performance at the beginning. Furthermore, the curves of both types of receivers deteriorate rapidly and converge to a BER that is much higher than the case without CSI estimation error.

As for the 16-point SCMA system, the phenomenon is nearly the same as the 4 point SCMA system. However, we can find out that the NB-LDPC coded receivers converge to a higher BER than B-LDPC coded receivers for a 16-point SCMA system. To conclude, the robustness of SG-JSG-SCMA system is worse than the individual receiver against the CSI estimation error because of more rapid BER deterioration. However, we can also see that the performance of both LDPC and NB-LDPC coded 4-point SG-JSG-SCMA are still better than the individual receivers even when variance of Δh is approximate to 0.1.

We also investigate the impact of channel estimation error on JTDD algorithm in a 200% overloading system. It can be observed from Fig. 19 that the robustness of JTDD algorithm

is approximately the same as the original NB-LDPC coded SG-JSG-SCMA, which they can both converge to a better BER performance than the B-LDPC coded receivers. From what have discussed above, the individual receiver is still more robust for a 200% overloading SCMA system even though it is not as significant as 150% overloading system.

VI. CONCLUSION

In this paper, we propose a sub-graph based JSG structure in the B-LDPC and NB-LDPC coded SCMA receiver. As demonstrated by the simulation results, our proposed SG-JSG-SCMA scheme can bring significant performance improvement compared to the existing receiver types with comparable computational complexity. Its performance improvement is mainly due to sufficient message exchange between SSG and LSG. By combining the SCMA trellis and NB-LDPC trellis, a JTR is introduced to represent the update of NB-LDPC coded SG-JSG-SCMA system. Based on such JTR, a JTDD algorithm using partial messages by selecting columns and truncating symbols in JTR is proposed to reduce the computational complexity of NB-LDPC coded SG-JSG-SCMA system. According to the simulation results and analysis, the JTDD performs well for both 150% and 200% overloading system with significant complexity reduction. To conclude, the proposed SG-JSG-SCMA is a promising receiver technique for LDPC coded SCMA system for 5G mMTC scenario.

REFERENCES

[1] J. Thompson *et al.*, "5G wireless communication systems: Prospects and challenges [Guest Editorial]," *IEEE Commun. Mag.*, vol. 52, no. 2, pp. 62–64, Feb. 2014.
[2] Y. Liu, Z. Ding, M. Elkashlan, and H. V. Poor, "Cooperative non-orthogonal multiple access with simultaneous wireless information and power transfer," *IEEE J. Sel. Areas Commun.*, vol. 34, no. 4, pp. 938–953, Apr. 2016.
[3] Y. Liang, X. Li, J. Zhang, and Z. Ding, "Non-orthogonal random access for 5G networks," *IEEE Trans. Wireless Commun.*, vol. 16, no. 7, pp. 4817–4831, Jul. 2017.
[4] H. Nikopour and H. Baligh, "Sparse code multiple access," in *Proc. IEEE Int. Symp. Pers. Indoor Mobile Radio Commun.*, Sep. 2013, pp. 332–336.
[5] R. Hoshyar, F. P. Wathan, and R. Tafazolli, "Novel low-density signature for synchronous CDMA systems over AWGN channel," *IEEE Trans. Signal Process.*, vol. 56, no. 4, pp. 1616–1626, Apr. 2008.
[6] J. van de Beek and B. M. Popovic, "Multiple access with low-density signatures," in *Proc. Global Telecommun. Conf. (GLOBECOM)*, Nov. 2009, pp. 1–6.
[7] R. Hoshyar, R. Razavi, and M. Al-Imari, "LDS-OFDM an efficient multiple access technique," in *Proc. IEEE Veh. Technol. Conf. (VTC-Spring)*, May 2010, pp. 1–5.
[8] M. Taherzadeh, H. Nikopour, A. Bayesteh, and H. Baligh, "SCMA codebook design," in *Proc. IEEE Veh. Technol. Conf. (VTC-Fall)*, Sep. 2014, pp. 1–5.
[9] F. Wei and W. Chen, "Low complexity iterative receiver design for sparse code multiple access," *IEEE Trans. Commun.*, vol. 65, no. 2, pp. 621–634, Feb. 2017.
[10] L. Tian, J. Zhong, M. Zhao, and L. Wen, "An optimized superposition constellation and region-restricted MPA detector for LDS system," in *Proc. IEEE Int. Conf. Commun. (ICC)*, May 2016, pp. 1–5.
[11] L. Yang, Y. Liu, and Y. Siu, "Low complexity message passing algorithm for SCMA system," *IEEE Commun. Lett.*, vol. 20, no. 12, pp. 2466–2469, Dec. 2016.
[12] J. Chen, Z. Zhang, S. He, J. Hu, and G. E. Sobelman, "Sparse code multiple access decoding based on a Monte Carlo Markov chain method," *IEEE Signal Process. Lett.*, vol. 23, no. 5, pp. 639–643, May 2016.
[13] H. Mu, Z. Ma, M. Alhaji, P. Fan, and D. Chen, "A fixed low complexity message pass algorithm detector for up-link SCMA system," *IEEE Wireless Commun. Lett.*, vol. 4, no. 6, pp. 585–588, Dec. 2015.
[14] Y. Wang and L. Qiu, "Edge selection-based low complexity detection scheme for SCMA system," in *Proc. IEEE Veh. Technol. Conf. (VTC-Fall)*, Sep. 2017, pp. 1–6.
[15] R. Razavi, M. Al-Imari, M. A. Imran, R. Hoshyar, and D. Chen, "On receiver design for uplink low density signature OFDM (LDS-OFDM)," *IEEE Trans. Commun.*, vol. 60, no. 11, pp. 3499–3508, Nov. 2012.
[16] L. Wen, R. Razavi, M. A. Imran, and P. Xiao, "Design of joint sparse graph for OFDM system," *IEEE Trans. Wireless Commun.*, vol. 14, no. 4, pp. 1823–1836, Apr. 2015.
[17] L. Wen and M. Su, "Joint sparse graph over GF(q) for code division multiple access systems," *IET Commun.*, vol. 9, no. 5, pp. 707–718, Mar. 2015.
[18] L. Wen, J. Lei, and M. Su, "Improved algorithm for joint detection and decoding on the joint sparse graph for CDMA systems," *IET Commun.*, vol. 10, no. 3, pp. 336–345, Mar. 2016.
[19] L. Wen *et al.*, "Joint sparse graph for FBMC/OQAM systems," *IEEE Trans. Veh. Technol.*, to be published, doi: 10.1109/TVT.2018.2810638.
[20] B. Xiao, K. Xiao, S. Zhang, Z. Chen, B. Xia, and H. Liu, "Iterative detection and decoding for SCMA systems with LDPC codes," in *Proc. IEEE Wireless Commun. Signal Process. Conf. (WCSP)*, Oct. 2015, pp. 1–5.
[21] K. Han, Z. Zhang, J. Hu, and J. Chen, "A high performance joint detection and decoding scheme for LDPC coded SCMA system," in *Proc. IEEE Globecom Workshops (GC Wkshps)*, Dec. 2017, pp. 1–6.
[22] Y. Du, B. Dong, Z. Chen, P. Gao, and J. Fang, "Joint sparse graph-detector design for downlink MIMO-SCMA systems," *IEEE Wireless Commun. Lett.*, vol. 6, no. 1, pp. 14–17, Feb. 2017.
[23] T. L. Narasimhan and A. Chockalingam, "Exit chart based design of irregular LDPC codes for large-MIMO systems," *IEEE Commun. Lett.*, vol. 17, no. 1, pp. 115–118, Jan. 2013.
[24] Y. Fang, G. Bi, Y. L. Guan, and F. C. M. Lau, "A survey on protograph LDPC codes and their applications," *IEEE Commun. Surveys Tuts.*, vol. 17, no. 4, pp. 1989–2016, 4th Quart., 2015.
[25] R. M. Tanner, "A recursive approach to low complexity codes," *IEEE Trans. Inf. Theory*, vol. IT-27, no. 5, pp. 533–547, Sep. 1981.
[26] R. Koetter, A. C. Singer, and M. Tüchler, "Turbo equalization," *IEEE Signal Process. Mag.*, vol. 21, no. 1, pp. 67–80, Jan. 2004.
[27] D. Declercq, "Non-binary decoder diversity for dense or locally-dense parity-check codes," *IEEE Trans. Commun.*, vol. 59, no. 3, pp. 729–739, Mar. 2011.
[28] S. Hongzin and J. R. Cruz, "Reduced-complexity decoding of Q-ary LDPC codes for magnetic recording," *IEEE Trans. Magn.*, vol. 39, no. 2, pp. 1081–1087, Mar. 2003.
[29] D. Declercq and M. Fossorier, "Decoding algorithms for nonbinary LDPC codes over GF(q)," *IEEE Trans. Commun.*, vol. 55, no. 4, pp. 633–643, Apr. 2007.
[30] E. Li, D. Declercq, and K. Gunnam, "Trellis-based extended min-sum algorithm for non-binary LDPC codes and its hardware structure," *IEEE Trans. Commun.*, vol. 61, no. 7, pp. 2600–2611, Jul. 2013.
[31] F. Wathan, R. Hoshyar, and R. Tafazolli, "Dynamic grouped chip-level iterated multiuser detection based on Gaussian forcing technique," *IEEE Commun. Lett.*, vol. 12, no. 3, pp. 167–169, Mar. 2008.
[32] Y. Weiss and W. Freeman, "Correctness of belief propagation in Gaussian graphical models of arbitrary topology," *Neural Comput.*, vol. 13, no. 10, pp. 2173–2200, Oct. 2001.
[33] T. J. Richardson, M. A. Shokrollahi, and R. L. Urbanke, "Design of capacity-approaching irregular low-density parity-check codes," *IEEE Trans. Inf. Theory*, vol. 47, no. 2, pp. 619–637, Feb. 2002.
[34] T. J. Richardson and R. L. Urbanke, "The capacity of low-density parity-check codes under message-passing decoding," *IEEE Trans. Inf. Theory*, vol. 47, no. 2, pp. 599–618, Feb. 2002.
[35] D. J. C. MacKay, S. T. Wilson, and M. C. Davey, "Comparison of constructions of irregular Gallager codes," *IEEE Trans. Commun.*, vol. 47, no. 10, pp. 1449–1454, Oct. 1999.
[36] D. J. C. MacKay, "Good error-correcting codes based on very sparse matrices," *IEEE Trans. Inf. Theory*, vol. 45, no. 2, pp. 399–431, Mar. 1999.
[37] S. ten Brink, "Convergence behavior of iteratively decoded parallel concatenated codes," *IEEE Trans. Commun.*, vol. 49, no. 10, pp. 1727–1737, Oct. 2001.
[38] S. ten Brink, G. Kramer, and A. Ashikhmin, "Design of low-density parity-check codes for modulation and detection," *IEEE Trans. Commun.*, vol. 52, no. 4, pp. 670–678, Apr. 2004.

[39] Z. Liu *et al.*, "Linear constellation precoding for OFDM with maximum multipath diversity and coding gains," *IEEE Trans. Commun.*, vol. 51, no. 3, pp. 416–427, Mar. 2003.
[40] G. V. Rangaraj, D. Jalihal, and K. Giridhar, "Exploiting multipath diversity in multiple antenna OFDM systems with spatially correlated channels," *IEEE Trans. Veh. Technol.*, vol. 54, no. 4, pp. 1372–1378, Jul. 2005.
[41] T. S. Rappaport, *Wireless Communications: Principles and Practice*, 2nd ed. Englewood Cliffs, NJ, USA: Prentice-Hall, 2001.
[42] I. A. Chatzigeorgiou, M. R. D. Rodrigues, I. J. Wassell, and R. A. Carrasco, "Comparison of convolutional and turbo coding for broadband FWA systems," *IEEE Trans. Broadcast.*, vol. 53, no. 2, pp. 494–503, Jun. 2007.
[43] Y. Du, B. Dong, Z. Chen, J. Fang, P. Gao, and Z. Liu, "Low-complexity detector in sparse code multiple access systems," *IEEE Commun. Lett.*, vol. 20, no. 9, pp. 1812–1815, Sep. 2016.

KE LAI received the B.Sc. degree in communication engineering from the National University of Defence Technology, Changsha, China, in 2016,where he is currently pursuing the M.Sc. degree with the Department of Communication Engineering, School of Electronic Science. His research interests include advanced multiple access techniques, channel coding, and physical-layer security.

LEI WEN received the B.Sc. degree in electrical information engineering from Xiangtan University, Xiangtan, China, in 2003, the M.Sc. degree in wireless communication systems from the National University of Defence Technology, Changsha, China, in 2006, and the Ph.D. degree in mobile communications from the 5G Innovation Centre, University of Surrey, U.K., in 2016. His research interests include channel coding and multi-user detection techniques, advanced multiple access techniques, and multi-carrier systems.

JING LEI received the B.Sc., M.Sc., and Ph.D. degrees from the National University of Defence Technology, Changsha, China, in 1990, 1994, and 2009, respectively. She was a Visiting Scholar with the School of Electronics and Computer Science, University of Southampton, U.K. She is currently a Distinguished Professor of the Department of Communications Engineering, College of Electronic Science, National University of Defence Technology, and the Leader of the Communication Coding Group. She has published many papers in various journals and conference proceedings and five books. Her research interests include information theory, LDPC, space–time coding, advanced multiple access technology, physical-layer security, wireless communication technology, and so on.

PEI XIAO (SM'11) was with Newcastle University and Queen's University Belfast. He also held positions at Nokia Networks, Finland. He is currently a Professor with the Institute for Communication Systems, Home of 5G Innovation Centre (5GIC), University of Surrey. He is also the Technical Manager of 5GIC, leading the research team at on the new physical-layer work area, and coordinating/supervising research activities across all the work areas within 5GIC. He has published extensively in the fields of communication theory and signal processing for wireless communications.

AMINE MAAREF (SM'12) received the Ph.D. degree in telecommunications from INRS-EMT, University of Quebec, in 2007. He was with Mitsubishi Electric Research Laboratories, Cambridge, MA, USA, as a Research Scientist, where he conducted advanced research in broadband mobile communications and was actively involved in 3GPP LTE/LTE-Advanced and WiMAX IEEE 802.16m standardization. He is currently an LTE and NR Technical Expert with Huawei Technologies, Ottawa, ON, Canada, focusing on 5G radio access design and NR technology promotion in 3GPP. Over the last 15 years, he has co-authored over 100 international peer-reviewed publications and standard contributions in the relevant areas, holds over 100 patents and pending patent applications, and received numerous prestigious awards for his outstanding research and scholarly achievements. He has been serving as an Editor of the IEEE TRANSACTIONS ON WIRELESS COMMUNICATIONS since 2014. He was a Guest Editor for several special issues of IEEE journals and magazines. He is a Founding Managing Editor of the IEEE 5G TECH FOCUS.

MUHAMMAD ALI IMRAN (M'03–SM'12) received the M.Sc. (Hons.) and Ph.D. degrees from Imperial College London, U.K., in 2002 and 2007, respectively. He has over 18 years of combined academic and industry experience, working primarily in the research areas of cellular communication systems. He is currently the Vice Dean of the Glasgow College UESTC and a Professor of communication systems with the School of Engineering, University of Glasgow. He is also an Affiliate Professor with The University of Oklahoma, USA, and a Visiting Professor with the 5G Innovation Centre, University of Surrey, U.K. He has been a principal/co-principal investigator on over č six million in sponsored research grants and contracts. He was a Co-Editor of two books *Access, Fronthaul and Backhaul Networks for 5G and Beyond* (IET) and *Energy Management in Wireless Cellular and Ad-hoc Networks* (Springer). He has authored/co-authored over 300 journal and conference publications and holds 15 patents. He has supervised over 30 successful Ph.D. graduates. He is a Senior Fellow of the Higher Education Academy, U.K. He received the Award of Excellence in recognition of his academic achievements, conferred by the President of Pakistan, the IEEE Comsoc's Fred Ellersick Award in 2014, the FEPS Learning and Teaching Award in 2014, the Sentinel of Science Award in 2016, the QS Stars Reimagine Education Award in 2016 for innovative teaching and VC's learning, and the Teaching Award from the University of Surrey. He was twice nominated for Tony Jean's Inspirational Teaching Award. He is a shortlisted finalist for The Wharton-QS Stars Awards in 2014.